THE GEOLOGICAL SOCIETY OF AMERICA®

Ultrapotassic rocks and xenoliths from South Tibet: Contrasting styles of interaction between lithospheric mantle and asthenosphere during continental collision

Bo Xu[1,2,3], William L. Griffin[2], Qing Xiong[2], Zeng-Qian Hou[3]*, Suzanne Y. O'Reilly[2], Zhen Guo[2], Norman J. Pearson[2], Yoann Gréau[2], Zhi-Ming Yang[3], and Yuan-Chuan Zheng[1]

[1]School of Earth Science and Mineral Resources, China University of Geosciences, Beijing 10083, China
[2]ARC Centre of Excellence for Core to Crust Fluid Systems (CCFS) and GEMOC, Department of Earth and Planetary Sciences, Macquarie University, Sydney, NSW 2109, Australia
[3]Institute of Geology, Chinese Academy of Geological Sciences, Beijing 100037, China

ABSTRACT

Widespread Miocene (24–8 Ma) ultrapotassic rocks and their entrained xenoliths provide information on the composition, structure, and thermal state of the sub-continental lithospheric mantle in southern Tibet during the India-Asia continental collision. The ultrapotassic rocks along the Lhasa block delineate two distinct lithospheric domains with different histories of depletion and enrichment. The eastern ultrapotassic rocks (89°E–92°E) reveal a depleted, young, and fertile lithospheric mantle ($^{87}Sr/^{86}Sr_t$ = 0.704–0.707 [t is eruption time]; Hf depleted-mantle model age [T_{DM}] = 377–653 Ma). The western ultrapotassic rocks (79°E–89°E) and their peridotite xenoliths (81°E) reflect a refractory harzburgitic mantle refertilized by ancient metasomatism (lavas: $^{87}Sr/^{86}Sr_t$ = 0.714–0.734; peridotites: $^{87}Sr/^{86}Sr_t$ = 0.709–0.716). These data integrated with seismic tomography suggest that upwelling asthenosphere was diverted away from the deep continental root beneath the western Lhasa block, but rose to shallower depths beneath a thinner lithosphere in the eastern part. Heating of the lithospheric mantle by the rising asthenosphere ultimately generated the ultrapotassic rocks with regionally distinct geochemical signatures reflecting the different nature of the lithospheric mantle.

INTRODUCTION

The collision between India and Asia formed the Tibetan Plateau and the Himalayan orogen (Harrison et al., 1992), affecting the evolution of atmosphere, hydrosphere, and global tectonics on Earth since the Cenozoic (e.g., Yin and Harrison, 2000; Kapp et al., 2008). The Lhasa block (South Tibet) is the tectonic unit closest to the India-Asia collision zone (e.g., Chung et al., 2005), and its lithospheric structure affects the nature of collision tectonics and lithosphere-asthenosphere interaction within this convergent regime.

Ultrapotassic rocks (UPRs) represent small-volume magmas derived from phlogopite-bearing subcontinental lithospheric mantle (SCLM; e.g., Foley et al., 1987). UPRs and their entrained xenoliths ± xenocrysts can provide information on the composition of the SCLM and its metasomatic modification during and after the continental collision (e.g., Prelević et al., 2008). In southern Tibet, UPRs occur widely within the Cenozoic rifts in the Lhasa block (Fig. 1) and have been interpreted as melts of enriched SCLM (e.g., Miller et al., 1999; Zhao et al., 2009, and references therein). However, the details of this interplay between the Lhasa lithosphere, the subducting Indian slab, and the asthenosphere during the India-Asia continental collision are still ambiguous.

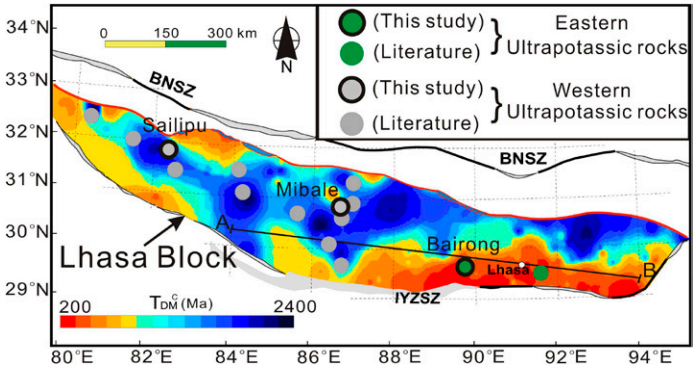

Figure 1. Hf-isotope contour map showing spatial variation of Hf model ages for granitoid rocks in Lhasa block (southern Tibet). Data and methods are described by Hou et al. (2015). Color bands indicate ranges of crustal model age (T_{DM}^{C}) values. Line A-B shows location of Figure 3B. IYZSZ—Indus–Yarlung-Zangbo suture zone; BNSZ—Bangong-Nujiang suture zone.

We present new whole-rock major- and trace-element analyses, in situ Sr-isotope data on clinopyroxene, and zircon U-Pb and Hf-isotope data for the mantle-derived UPRs in the Lhasa block and compare them with recent seismic tomography from southern Tibet. These data provide a picture of the lithospheric mantle beneath the Lhasa block, revealing (1) two distinct lithospheric mantle domains and (2) contrasting styles of interaction between lithospheric mantle and asthenosphere along the India-Asia collision zone.

GEOLOGICAL SETTING AND SAMPLES

The Tibetan-Himalayan orogenic system formed by collision between the Indian and Asian continents during the Cenozoic (e.g., Yin and Harrison, 2000). The Tibetan Plateau is composed of three continental terranes: from south to north, the Lhasa, Qiangtang, and Songpan-Ganze blocks. The Lhasa block is bounded by the Bangong-Nujiang suture zone in the north and the Yarlung Zangbo suture zone in the south (Fig. 1). The Lhasa continental fragment was rifted from eastern Gondwana, moved across the Tethyan Ocean during the early Mesozoic, and collided with the Qiangtang block in the early Cretaceous (e.g., Yin and Harrison, 2000). The long-term subduction of Neo-Tethyan slabs beneath the Lhasa block built two juvenile magmatic arcs on this core (e.g., Zhu et al., 2011).

After the closure of the Neo-Tethyan Ocean, the Greater Indian plate subducted northwards beneath South Tibet, generating a nearly east-west belt of Miocene UPRs within the Lhasa block (Fig. 1). This UPR belt

*E-mail: Houzengqian@126.com

decreases in age from 24 Ma to 8 Ma from west to east; it extends from the city of Shiquanhe at ~79°E, through Sailipu, Bongba, Xunba, Mibale, Maiga, Zhabuye, Chazi, Bairong, and Jiama at ~92°E (Table DR1 in the GSA Data Repository[1]; e.g., Zhao et. al., 2009). Most UPRs in the west (79°E–89°E) intruded a Precambrian subterrane with old Hf-isotope crustal model ages (Fig. 1), while rare ultrapotassic minettes from the eastern Gangdese magmatic arc intrude younger crust (89°E–92°E; Fig. 1). The western UPRs (WUPRs) occur as lava flows unconformably overlying Cretaceous–Paleogene volcanic-sedimentary sequences (e.g., Miller et al., 1999). The eastern UPRs (EUPRs) crop out as dikes at the Gangdese porphyry Cu deposits (Bairong and Jiama; Yang et al., 2016). This study focuses on the Sailipu (82°E), Mibale (86°E), and Bairong (90°E) UPRs (Fig. DR1), spread along the whole UPR belt (Fig. 1). Detailed sample descriptions are given in the Data Repository.

RESULTS

Ultrapotassic magmas pass through the lithospheric mantle and crust during eruption, potentially resulting in wall-rock contamination and fractionation. In order to define primary magma compositions, we have compiled data on 127 UPRs from the Lhasa block with high contents of MgO (6–15 wt%), Ni (94–527 ppm), and Cr (123–728 ppm) but low contents of SiO_2 (40–59 wt%) (Table DR1). The occurrence of mantle xenoliths in these lavas indicates that they ascended rapidly (O'Reilly et al., 2009), suggesting limited interaction with continental crust (Liu et al., 2011). Then we used the Sr- and Hf-isotope compositions of the least-contaminated rocks and their clinopyroxene and zircon to examine the mantle sources of the magmas. Analytical methods are described in the Data Repository.

Whole-Rock Major- and Trace-Element Compositions

In the EUPR belt, the Bairong minettes have intermediate SiO_2 but high MgO, CaO, and K_2O, with Mg# [100 × molar Mg/(Mg + Fe)] of 70–75 and $K_2O/Na_2O > 2$ (Table DR2). Their whole-rock trace-element compositions (Table DR2) are enriched in large-ion lithophile elements (LILEs) and light rare earth elements (LREEs) relative to the primitive mantle, but depleted in high-field-strength elements (Fig. DR2 in the Data Repository). In contrast, the WUPRs show a wider range of SiO_2 and lower CaO. The WUPRs are also extremely enriched in LILEs and LREEs, with significant negative anomalies in Nb, Ta, and Ti (Nb/Pb = 0.3–5.9; Fig. DR3).

Zircon U-Pb Ages and Hf-Isotope Compositions

Zircons extracted from the Bairong minettes are euhedral prisms or subhedral fragments <80 μm in length and show oscillatory or sector zoning with no inherited cores or inclusions (Fig. DR4). U-Pb ages on 12 grains from sample BR14-1 and 10 grains from BR14-4 (Table DR3) give weighted average $^{206}Pb/^{238}U$ ages of 11.8 ± 0.2 Ma (mean square of weighted deviates [MSWD] = 3.4, 1σ) and 11.4 ± 0.3 Ma (MSWD = 12, 1σ), respectively (Fig. DR5). The Th/U ratios and REE patterns of these grains are consistent with an igneous origin. Lu-Hf analyses of the same grains (Table DR4) show low $^{176}Lu/^{177}Hf$ ratios (<0.00189) and high $^{176}Hf/^{177}Hf$ (0.28279–0.28299), giving positive $\varepsilon_{Hf}(t)$ values (+7.9 to +0.8; Fig. 2A), and young depleted-mantle model ages (T_{DM} = 377–653 Ma) and crustal model ages (T_{DM}^C = 588–1047 Ma). However, zircons from WUPRs have old T_{DM}^C ages, ranging from 1001 to 2471 Ma (Liu et al., 2014; Tian et al., in press).

In Situ Clinopyroxene Sr-Isotope Compositions

In situ Sr-isotope analyses (n = 109) have been carried out on clinopyroxene phenocrysts from the Sailipu, Mibale, and Bairong UPRs and on clinopyroxene grains in the Sailipu peridotite xenoliths entrained by the UPRs (Tables DR5 and DR6). Clinopyroxenes in the WUPRs (Sailipu at ~82°E and Mibale at ~86°E) show radiogenic $^{87}Sr/^{86}Sr_t$ (t is eruptive time) (0.714–0.734 and 0.709–0.716, respectively; Fig. 2B). Clinopyroxenes from the Bairong UPRs (at ~90°E) in the eastern segment have much less radiogenic signatures ($^{87}Sr/^{86}Sr_t$ = 0.704–0.709). The *in situ* results are consistent with the whole-rock Sr-isotope data, which show more scatter and radiogenic ratios in the west versus a narrow and unradiogenic range in the east (Fig. 2B).

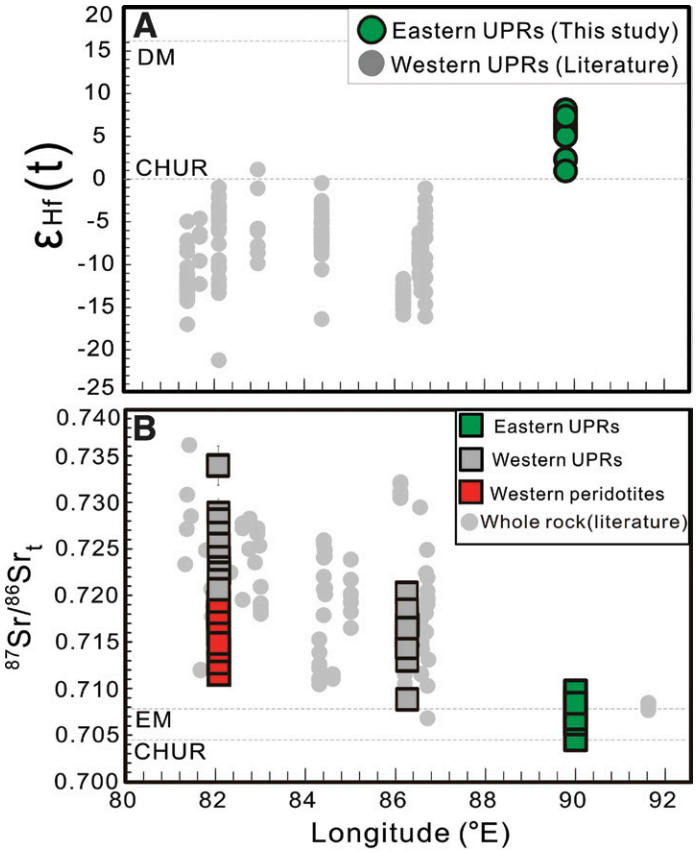

Figure 2. A: Plot of zircon $\varepsilon_{Hf}(t)$ versus longitude in Lhasa ultrapotassic rocks (UPRs) (southern Tibet). B: Distribution of clinopyroxene and whole-rock $^{87}Sr/^{86}Sr_t$ versus longitude in Lhasa block. DM—depleted-mantle value; CHUR—chondritic uniform reservoir; EM—enriched mantle.

DISCUSSION

Origin of the Lhasa Ultrapotassic Rocks

The UPRs of the Lhasa block have been argued to be derived from low-degree partial melting of hydrous, enriched, phlogopite-bearing SCLM (e.g., Miller et al., 1999, and references therein), and/or pyroxenite-bearing mantle (Huang et al., 2015). The presence of phlogopite-bearing peridotite xenoliths in these UPRs (Liu et al., 2011) also suggests the involvement of a mantle source in the genesis of the ultrapotassic magmas, and our modeling indicates low-degree melting of a garnet peridotite source (Fig. DR3).

The Bairong ultrapotassic dikes in the EUPR belt and UPRs in the western belt have high contents of MgO (6.0–15.0 wt%; Mg# >70), Cr (123–728 ppm), and Ni (94–527 ppm; Fig. DR2), suggesting that they are primary melts derived from upper-mantle peridotites (Frey et al., 1978) and experienced little crustal assimilation. However, all of the Lhasa UPRs show patterns of incompatible trace elements similar to those of Mediterranean UPRs, which are considered to have both pelagic and terrigenous components (Fig. DR2; e.g., Zhao et al., 2009; Prelević et al., 2008;

[1]GSA Data Repository item 2017013, methods, literature data sources, Tables DR1–DR6, and Figures DR1–DR5, is available online at www.geosociety.org/pubs/ft2017.htm or on request from editing@geosociety.org.

Tommasini et al., 2011, and references therein). These features may reflect the involvement of hydrous, K-rich metasomatic components introduced into the lithospheric mantle by subduction or by crustal delamination (e.g., Wyllie and Sekine, 1982). Therefore, the primary magmatic compositions of the Lhasa UPRs may reflect the nature of their mantle source.

Two Distinct Lithospheric Mantle Domains Revealed by UPRs in the Lhasa Block

Hf- and Nd-isotope mapping of the exposed Miocene surface rocks and Hf isotopes in granulite xenoliths have revealed ancient crustal signatures within the Lhasa block (Hou et al., 2015; Wang et al., 2016). The EUPRs are located in the Gangdese magmatic arc (southeastern quarter of the Lhasa block) where crustal rocks have juvenile Hf-isotope signatures, while most UPRs occur in the western part of the Lhasa block, with ancient Hf-isotope compositions (Fig. 1). The crustal differences between the western and eastern Lhasa sub-blocks suggest that the underlying SCLM of both regions may be also distinctive.

Inherited olivine xenocrysts in the WUPRs have high Mg# (up to 92.7; Guo et al., 2015), and the Sailipu harzburgite xenoliths have high Cr# in spinel (up to 73; Liu et al., 2011), indicating sampling of refractory SCLM from the western Lhasa block. The high-MgO WUPRs have igneous zircons with low $\varepsilon_{Hf}(t)$ ranging from −21.2 to +1.1 (Fig. 2A), suggesting that the magmatic source of the UPRs has been isolated from the convective mantle for >1 b.y. Clinopyroxene phenocrysts from the Sailipu UPRs (~82°E) show high $^{87}Sr/^{86}Sr_t$ (0.714–0.734), and clinopyroxenes from the entrained peridotite xenoliths have $^{87}Sr/^{86}Sr_t$ of 0.714–0.719. The Mibale UPRs (~86°E) are also characterized by high $^{87}Sr/^{86}Sr_t$ (0.709–0.716) in clinopyroxene. The "enriched" isotopic nature of the magmatic source beneath the western Lhasa block is supported by whole-rock Sr-Nd isotopic data from high-MgO UPRs [$^{87}Sr/^{86}Sr_t$ = 0.71025–0.73762; $\varepsilon_{Nd}(t)$ = −16.9 to −8.4; T_{DM} = 1193–4049 Ma; Fig. 2B; e.g., Zhao et al., 2009] and their olivine xenocrysts [$^{87}Sr/^{86}Sr_t$ = 0.7259; $\varepsilon_{Nd}(t)$ = −16.6; Miller et al., 1999]. These Hf-Sr-Nd isotopic signatures can be explained by ancient metasomatic addition of components with low Lu/Hf and Sm/Nd but high Rb/Sr to a depleted SCLM (mean Rb/Sr = 0.67; Fig. DR3). This interpretation is consistent with the high contents of incompatible elements in the WUPRs (Table DR2).

The superposition of enriched elemental signatures on the refractory SCLM suggests that the western Lhasa block has an ancient (at least Paleoproterozoic) keel of cool and stable SCLM that was metasomatically refertilized by components derived from subducting slabs or the underlying asthenosphere. In the southeastern Lhasa block, by contrast, the clinopyroxenes from the Bairong UPRs (~89°E) show $^{87}Sr/^{86}Sr_t$ of 0.704–0.707 (Fig. 2B), higher than that of the bulk silicate earth but much lower than those of the WUPRs and their xenoliths (Fig. 2B). The zircon Hf-isotope data (Fig. 2A) also suggest the presence of young juvenile mantle beneath the eastern belt of UPRs. In addition, the EUPRs have higher whole-rock CaO contents but lower contents of LREEs (Fig. DR2; Table DR2) and LILEs (Fig. DR2; Table DR2) than the WUPRs, suggesting a younger, less metasomatized SCLM source for the EUPRs.

Collectively, the WUPRs reveal a refractory but refertilized SCLM of Archean to Paleoproterozoic age, while the data from the EUPRs indicate a more fertile, isotopically "depleted" and juvenile lithospheric mantle beneath the southeastern Lhasa block.

Contrasting Styles of Interaction between Lithospheric Mantle and Asthenosphere during the India-Asia Collision

After the onset of the India-Asia collision, the widespread Miocene UPRs in the Lhasa block were generated by heating of the SCLM source, caused mainly by a transition in tectonic regime (from compressional to extensional) during the Indian slab breakoff or the tearing or thinning of the South Tibetan lithospheric root (e.g., Miller et al., 1999, and references therein). This resulted in the upwelling of asthenosphere during the Indian continental convergence, and mechanical and thermal interaction between the asthenosphere and the overlying lithosphere of the Lhasa block. Lateral variations in the nature of the Lhasa SCLM and/or in the subduction mode of the Indian continental slab resulted in different styles of interaction at the mantle scale.

The difference in upper-mantle composition and thermal state beneath the western and eastern parts of the UPR belt is visible in recent high-resolution seismic-tomography images of the Lhasa block (Fig. 3; Liang et al., 2016). An elongated low-velocity anomaly is observed beneath the belt of EUPRs, extending from the base of the crust to >300 km depth and from 89°E to 93°E–94°E. This low-velocity zone is interpreted as a hot upper-mantle segment. The relatively weak seismic anisotropy beneath the EUPR belt is interpreted to reflect asthenospheric upwelling, which resulted in a high geotherm (Chen et al., 2015). In contrast, the western part of the block shows higher seismic velocities extending to depths of 150–200 km, consistent with the presence of a cooler mantle root.

This difference in S-wave velocity (Vs) (Fig. 3) is related to both fertility and age, as the increase in fertility from Paleoproterozoic-Archean to Phanerozoic SCLM corresponds to an increase in density of 2%–2.3% and a decrease in Vs of 1.0%–1.4% (Griffin et al., 2009). The typical thickness of the depleted ancient (Archean) SCLM is ~200 km, resulting in low geotherms; the fertile young (Phanerozoic) SCLM is typically <100 km thick with high geotherms (O'Reilly and Griffin, 2006; Griffin et al., 2009, and references therein). Thus, the seismic data are consistent with the geochemical evidence for young and fertile lithosphere in the eastern part. The thick, cool and refractory SCLM mapped beneath the WUPR belt by seismic data is similarly consistent with the geochemical evidence that this SCLM root is ancient, depleted, and only partly refertilized.

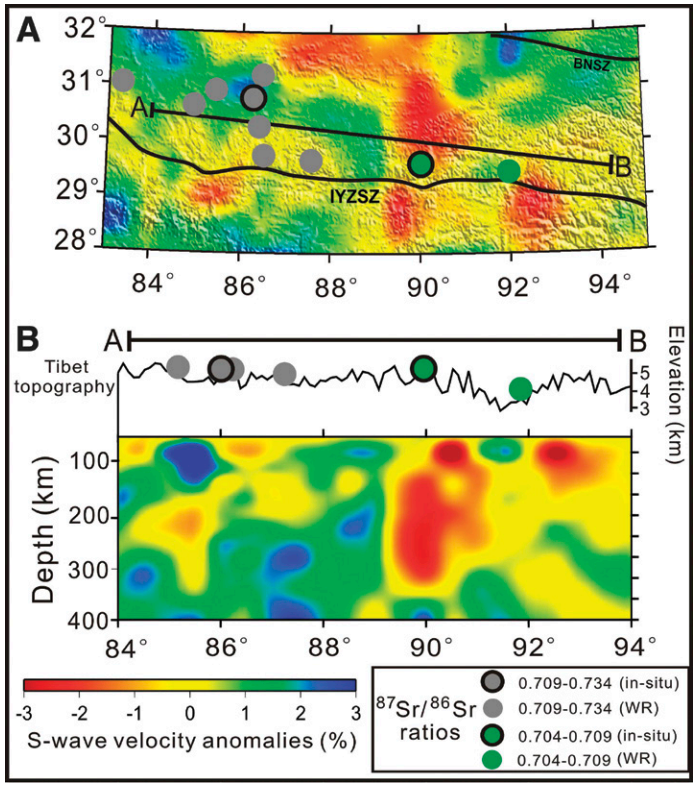

Figure 3. S-wave velocity structure beneath the Lhasa terrane (southern Tibet) from seismic tomography (Liang et al., 2016) with ultrapotassic rock locations (gray and green spots). A: Vs averaged over depths of 50–253 km. IYZSZ—Indus–Yarlung-Zangbo suture zone; BNSZ—Bangong-Nujiang suture zone. B: West-to-east (A to B) vertical cross section of Vs model. WR—whole rock.

This abrupt transition in mantle structure at ~89°E (Fig. 3) beneath the Lhasa block would have a significant effect on magma dynamics during the collision. Upwelling asthenosphere would be diverted away from the western SCLM keel but could rise to shallow depths in the absence of a keel beneath the southeastern Lhasa block. Heating would induce melting in both mantle domains, but at different depths, producing the observed differences in geochemical signatures.

CONCLUSIONS

Integration of geochemical, isotopic, and geophysical studies of post-collisional UPRs in southern Tibet delineates two distinct lithospheric mantle domains. The western belt is underlain by a metasomatized, refractory, thick and cool lithospheric mantle of Paleoproterozoic to Archean age; the eastern belt is underlain by a more fertile, thin, hot and juvenile mantle lithosphere. This structure has produced contrasting styles of interaction between the lithospheric mantle and the asthenosphere during continental collision.

ACKNOWLEDGMENTS

We thank Rosanna Murphy and Will Powell (CCFS/GEMOC) for their assistance with isotopic analyses, and Xiao-Feng Liang (Chinese Academy of Sciences) for seismic data. The study was jointly supported by The National Key Research and Development Project of China (2016YFC0600310), National Science Foundation of China (41320104004), ARC Centre of Excellence grants (SYO'R and WLG), and scholarships from the Chinese Scholarship Council and Macquarie University. The study used instrumentation funded by ARC Linkage Infrastructure, Equipment and Facilities (LIEF) and Department of Education and Training (DEST) Systemic Infrastructure Grants. We acknowledge the handling of editor J.B. Murphy and constructive comments from Dejan Prelević, Iain Neill, and an anonymous reviewer. This is contribution 862 from the ARC Centre of Excellence for Core to Crust Fluid Systems (http://www.ccfs.mq.edu.au), and contribution 1118 from the GEMOC ARC National Key Centre (http://www.gemoc.mq.edu.au).

REFERENCES CITED

Chen, Y., Li, W., Yuan, X., Badal, J., and Teng, J., 2015, Tearing of the Indian lithospheric slab beneath southern Tibet revealed by SKS-wave splitting measurements: Earth and Planetary Science Letters, v. 413, p. 13–24, doi:10.1016/j.epsl.2014.12.041.

Chung, S.-L., Chu, M.-F., Zhang, Y., Xie, Y., Lo, C.-H., Lee, T.-Y., Lan, C.-Y., Li, X., Zhang, Y.Q., and Wang, Y., 2005, Tibetan tectonic evolution inferred from spatial and temporal variations in post-collisional magmatism: Earth-Science Reviews, v. 68, p. 173–196, doi:10.1016/j.earscirev.2004.05.001.

Foley, S.F., Venturelli, G., Green, D.H., and Toscani, L., 1987, The ultrapotassic rocks: Characteristics, classification and constraints for petrogenetic models: Earth-Science Reviews, v. 24, p. 81–134, doi:10.1016/0012-8252(87)90001-8.

Frey, F.A., Green, D.H., and Roy, S.D., 1978, Integrated models of basalt petrogenesis: A study of quartz tholeiites to olivine melilitites from south eastern Australia utilizing geochemical and experimental petrological data: Journal of Petrology, v. 19, p. 463–513, doi:10.1093/petrology/19.3.463.

Griffin, W.L., O'Reilly, S.Y., Afonso, J.C., and Begg, G.C., 2009, The composition and evolution of lithospheric mantle: A re-evaluation and its tectonic implications: Journal of Petrology, v. 50, p. 1185–1204, doi:10.1093/petrology/egn033.

Guo, Z.F., Wilson, M., Zhang, M., Cheng, Z., and Zhang, L., 2015, Post-collisional ultrapotassic mafic magmatism in South Tibet: Products of partial melting of pyroxenite in the mantle wedge induced by roll-back and delamination of the subducted Indian continental lithosphere slab: Journal of Petrology, v. 56, p. 1365–1406, doi:10.1093/petrology/egv040.

Harrison, T.M., Copeland, P., Kidd, W.S.F., and Yin, A., 1992, Raising Tibet: Science, v. 255, p. 1663–1670, doi:10.1126/science.255.5052.1663.

Hou, Z.Q., et al., 2015, Lithospheric architecture of the Lhasa terrane and its control on ore deposits in the Himalayan-Tibetan orogen: Economic Geology and the Bulletin of the Society of Economic Geologists, v. 110, p. 1541–1575, doi:10.2113/econgeo.110.6.1541.

Huang, F., Chen, J.L., Xu, J.F., Wang, B.D., and Li, J., 2015, Os-Nd-Sr isotopes in Miocene ultrapotassic rocks of southern Tibet: Partial melting of a pyroxenite-bearing lithospheric mantle?: Geochimica et Cosmochimica Acta, v. 163, p. 279–298, doi:10.1016/j.gca.2015.04.053.

Kapp, P., Taylor, M., Stockli, D., and Ding, L., 2008, Development of active low-angle normal fault systems during orogenic collapse: Insight from Tibet: Geology, v. 36, p. 7–10, doi:10.1130/G24054A.1.

Liang, X.F., et al., 2016, 3D imaging of subducting and fragmenting Indian continental lithosphere beneath southern and central Tibet using body-wave finite-frequency tomography: Earth and Planetary Science Letters, v. 443, p. 162–175, doi:10.1016/j.epsl.2016.03.029.

Liu, C.Z., Wu, F.Y., Chung, S.L., and Zhao, Z.D., 2011, Fragments of hot and metasomatized mantle lithosphere in Middle Miocene ultrapotassic lavas, southern Tibet: Geology, v. 39, p. 923–926, doi:10.1130/G32172.1.

Liu, D., et al., 2014, Postcollisional potassic and ultrapotassic rocks in southern Tibet: Mantle and crustal origins in response to India–Asia collision and convergence: Geochimica et Cosmochimica Acta, v. 143, p. 207–231, doi:10.1016/j.gca.2014.03.031.

Miller, C., Schuster, R., Kltzli, U., Frank, W., and Purtscheller, F., 1999, Post-collisional potassic and ultrapotassic magmatism in SW Tibet: Geochemical and Sr-Nd-Pb-O isotopic constraints for mantle source characteristics and petrogenesis: Journal of Petrology, v. 40, p. 1399–1424, doi:10.1093/petroj/40.9.1399.

O'Reilly, S.Y., and Griffin, W.L., 2006, Imaging global chemical and thermal heterogeneity in the subcontinental lithospheric mantle with garnets and xenoliths: Geophysical implications: Tectonophysics, v. 416, p. 289–309, doi:10.1016/j.tecto.2005.11.014.

O'Reilly, S.Y., Zhang, M., Griffin, W.L., Begg, G., and Hronsky, J., 2009, Ultradeep continental roots and their oceanic remnants: A solution to the geochemical "mantle reservoir" problem?: Lithos, v. 112, p. 1043–1054, doi:10.1016/j.lithos.2009.04.028.

Prelević, D., Foley, S.F., Romer, R., and Conticelli, S., 2008, Mediterranean Tertiary lamproites derived from multiple source components in postcollisional geodynamics: Geochimica et Cosmochimica Acta, v. 72, p. 2125–2156, doi:10.1016/j.gca.2008.01.029.

Tian, S.H., Yang, Z.S., Hou, Z.Q., Mo, X.X., Hu, W.J., Zhao, Y., and Zhao, X.Y., 2015, Subduction of the Indian lower crust beneath southern Tibet revealed by the post-collisional potassic and ultrapotassic rocks in SW Tibet: Gondwana Research, doi:10.1016/j.gr.2015.09.005.

Tommasini, S., Avanzinelli, R., and Conticelli, S., 2011, The Th/La and Sm/La conundrum of the Tethyan realm lamproites: Earth and Planetary Science Letters, v. 301, p. 469–478, doi:10.1016/j.epsl.2010.11.023.

Wang, R., Collins, W.J., Weinberg, R.F., Li, J.X., Li, Q.Y., He, W.Y., Richards, J.P., Hou, Z., Zhou, L.M. and Stern, R.A., 2016, Xenoliths in ultrapotassic volcanic rocks in the Lhasa block: Direct evidence for crust–mantle mixing and metamorphism in the deep crust: Contributions to Mineralogy and Petrology, v. 171, 62, doi:10.1007/s00410-016-1272-6.

Wyllie, P.J., and Sekine, T., 1982, The formation of mantle phlogopite in subduction zone hybridization: Contributions to Mineralogy and Petrology, v. 79, p. 375–380, doi:10.1007/BF01132067.

Yang, Z.M., Goldfarb, R., and Chang, Z.S., 2016, Generation of post-collisional porphyry copper deposits in southern Tibet triggered by subduction of the Indian continental plate: Society of Economic Geologists Special Publication 19, 279–300.

Yin, A., and Harrison, T.M., 2000, Geologic evolution of the Himalayan-Tibetan orogen: Annual Review of Earth and Planetary Sciences, v. 28, p. 211–280, doi:10.1146/annurev.earth.28.1.211.

Zhao, Z., Mo, X., Dilek, Y., Niu, Y., DePaolo, D.J., Robinson, P., Zhu, D., Sun, C., Dong, G., and Zhou, S., 2009, Geochemical and Sr-Nd-Pb-O isotopic compositions of the post-collisional ultrapotassic magmatism in SW Tibet: Petrogenesis and implications for India intra-continental subduction beneath southern Tibet: Lithos, v. 113, p. 190–212, doi:10.1016/j.lithos.2009.02.004.

Zhu, D.C., Zhao, Z.D., Niu, Y., Mo, X.X., Chung, S.L., Hou, Z.Q., Wang, L.Q., and Wu, F.Y., 2011, The Lhasa terrane: Record of a micro-continent and its histories of drift and growth: Earth and Planetary Science Letters, v. 301, p. 241–255, doi:10.1016/j.epsl.2010.11.005.

Manuscript received 10 August 2016
Revised manuscript received 10 October 2016
Manuscript accepted 11 October 2016

Printed in USA